

Excited State Dynamics and Dye–Dye Interactions in Dye-Coated Gold Nanoparticles with Varying Alkyl Spacer Lengths

Michał Malicki, Joel M. Hales, Mariacristina Rumi, Stephen Barlow, LaKeisha McClary, Seth R. Marder, and Joseph W. Perry

School of Chemistry and Biochemistry and Center for Organic Photonics and Electronics, Georgia Institute of Technology, Atlanta, GA

Supporting Information

- S2** Synthesis
- S11** TEM Analysis
- S13** FT-IR Analysis of Mixed-ligand Au NPs
- S14** Calculations of Residual Oleylamine in AuS-C3-TPD and AuS-C12-TPD Based on ¹H NMR Measurements
- S15** Calculation of the Average Dye-dye Distance Ratio for AuS-C3-TPD and AuS-C12-TPD
- S16** UV-Vis Absorption Spectra and Analysis of the Mixed-ligand Au NP Systems
- S17** Time-Correlated Single Photon Counting Measurements
- S22** Femtosecond Transient Absorption Measurements
- S29** References

Synthesis

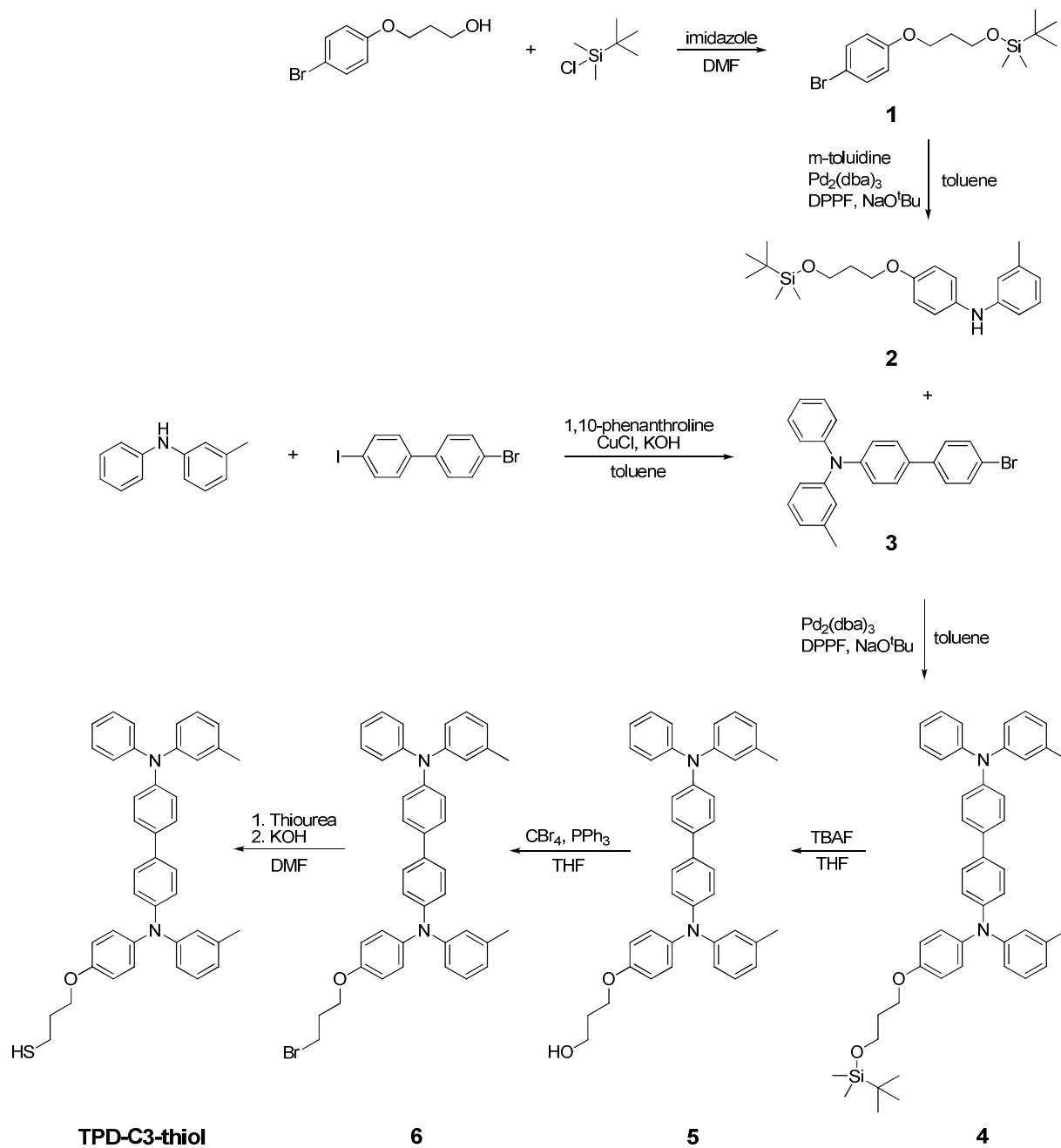


Fig. S1 Synthesis of TPD-C3-thiol

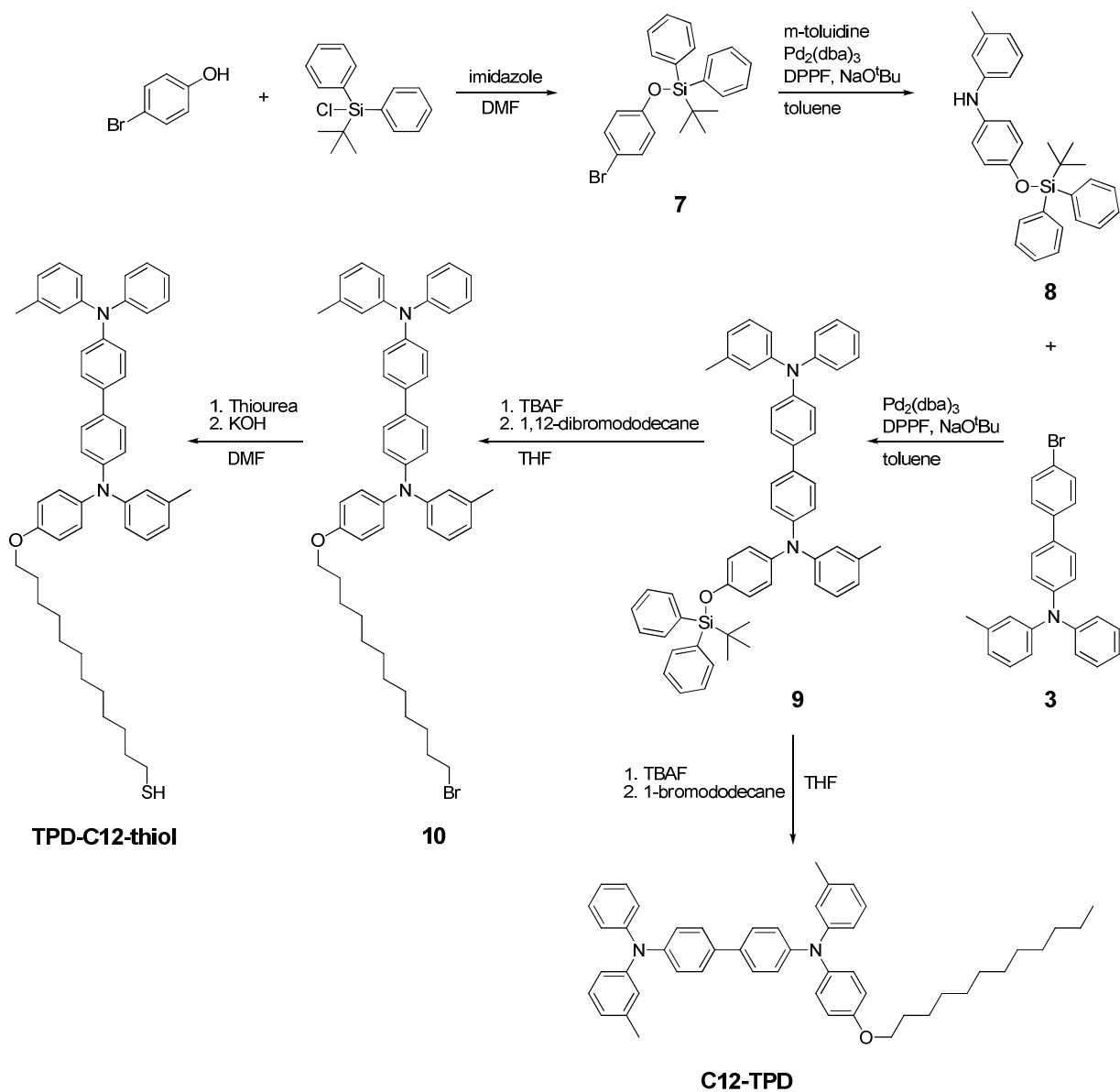


Fig. S2 Synthesis of TPD-C12-thiol and C12-TPD

3-(4-Bromo-phenoxy)-propan-1-ol, 4'-bromo-4-iodo-biphenyl, **1**, **2**, **3**, **4**, and **5** were prepared according to procedures published in ref. 1, and **7** was prepared according to the procedure described in ref. 2.

N-[4-(3-Bromopropoxy)]phenyl]-*N'*-phenyl-*N,N'*-di(*m*-tolyl)-biphenyl-4,4'-diamine (**6**)

5 (6.48 g, 11.0 mmol) was added to a dry round-bottomed flask containing dry THF (60 mL). The mixture was stirred and bubbled with argon gas for 20 min. Next triphenylphosphine (5.64 g, 21.5 mmol) and carbon tetrabromide (7.13 g, 21.5 mmol) were added and the mixture was stirred at room temperature for 1 h. Next the flask was opened to air and THF was evaporated under reduced pressure. The product was purified by column chromatography using hexane / dichloromethane (7:3). Evaporating the solvent under reduced pressure yielded the pure product (6.1 g, 85%). ¹H NMR (250 MHz, acetone-*d*₆) δ (ppm) 7.39-7.47 (m, 4H), 6.77-7.27 (m, 21H), 4.08 (t, *J* = 5.8 Hz, 2H), 3.64 (t, *J* = 6.5 Hz, 2H), 2.27 (quint, *J* = 6.0 Hz, 2H), 2.19 (s, 3H), 2.18 (s, 3H); ¹³C{¹H} NMR (62.5 MHz, acetone-*d*₆) δ (ppm) 155.49, 147.89, 147.75, 147.62, 147.21, 146.66, 140.68, 138.95, 138.75, 134.47, 133.38, 129.22, 129.14, 129.00, 127.19, 126.95, 126.91, 124.88, 123.99, 123.81, 123.11, 122.69, 122.44, 121.51, 120.44, 115.41, 65.48, 32.33, 30.07, 20.59, 20.54;* Anal. Calcd for C₄₁H₃₇BrN₂O: C, 75.34; H, 5.71; N, 4.29, Found C, 75.30; H, 5.68; N, 4.22; HRMS-EI (*m/z*): calcd for C₄₁H₃₇BrN₂O (M⁺), 652.2089; found, 652.2078.

N-[4-(3-Mercaptopropoxy)]phenyl]-*N'*-phenyl-*N,N'*-di(*m*-tolyl)-biphenyl-4,4'-diamine (**TPD-C3-thiol**)

6 (4.84 g, 7.41 mmol) was dissolved in DMF (100 mL) in a round-bottomed flask under an argon atmosphere. Thiourea (1.41 g, 18.5 mmol) was added and the mixture was heated up to 90 °C and stirred for 4 hours. Next potassium hydroxide (15.0 g, 230 mmol) in water (50 mL) was added and the reaction mixture was stirred for additional 10 hours. After that time the reaction mixture was neutralized by addition of 1M sulfuric acid and the product was extracted with diethyl ether.

* Two aromatic carbon signals are missing most likely due to an overlap.

The organic phase was washed with diluted hydrochloric acid after which ether was evaporated under reduced pressure and the solid residue was dissolved in dichloromethane (150 mL). The solution was dried over magnesium sulfate and filtered. The product was purified by column chromatography using dichloromethane / hexane (2:3). Evaporating the solvent under reduced pressure yielded the desired product (3.06 g, 68%). ^1H NMR (500 MHz, acetone- d_6) δ (ppm) 7.52 (d, $J = 8.7$ Hz, 2H), 7.50 (d, $J = 8.7$ Hz, 2H), 7.26-7.30 (m, 2H), 7.18 (t, $J = 7.7$ Hz, 1H), 7.14 (t, $J = 7.8$ Hz, 1H), 6.98-7.08 (m, 9H), 6.81-6.95 (m, 8H), 4.10 (t, $J = 6.1$ Hz, 2H), 2.72 (app. q, $J = 7.1$ Hz, 2H), 2.24 (s, 3H), 2.23 (s, 3H), 2.06 (app. quint, $J = 6.9$ Hz, 2H), 1.81 (t, $J = 8.1$ Hz, 1H); ^{13}C { ^1H } NMR (125 MHz, acetone- d_6) δ (ppm) 157.72, 149.86, 149.71, 149.58, 149.22, 148.63, 142.42, 140.93, 140.72, 136.46, 135.30, 131.17, 131.08, 130.92, 129.22, 128.88, 128.83, 126.83, 125.93, 125.80, 125.73, 125.69, 125.02, 124.66, 124.27, 123.44, 122.32, 117.31, 67.79, 35.36, 22.53, 22.47, 22.42; Anal. Calcd for $\text{C}_{41}\text{H}_{38}\text{N}_2\text{OS}$: C, 81.15; H, 6.31; N, 4.62; S, 5.28, Found C, 81.06; H, 6.22; N, 4.61; S, 5.04; HRMS-EI (m/z): calcd for $\text{C}_{41}\text{H}_{38}\text{N}_2\text{OS}$ (M^+), 606.2705; found, 606.2702.

N-[4-(*tert*-Butyldiphenylsilyloxy)phenyl]-3-methylaniline (**8**)

7 (15.00 g, 36.5 mmol) was added to a Schlenk tube containing anhydrous toluene (10 mL), $\text{Pd}_2(\text{dba})_3$ (0.57 g, 0.62 mmol), DPPF (0.69 g, 1.24 mmol), and NaO^tBu (8.76 g, 91.2 mmol). *m*-Toluidine (5.5 mL, 51.3 mmol) was then slowly added to the stirring reaction mixture. The reaction was sealed under inert atmosphere, heated to 95 °C, and stirred for 20 h. The product was purified by column chromatography using hexanes / diethyl ether (30:1) as eluent. Evaporating the solvent under reduced pressure yielded the desired product as a viscous liquid (13.00 g, 82%). ^1H NMR (500 MHz, CD_2Cl_2) δ (ppm) 7.79 (d, $J = 6.6$ Hz, 4H), 7.50 (t, $J = 7.4$

Hz, 2H), 7.44 (dd, $J = 7.5$ Hz, 6.9 Hz, 4H), 7.10 (t, $J = 7.8$ Hz, 1H), 6.90 (d, $J = 8.8$ Hz, 2H), 6.76 (d, $J = 8.9$ Hz, 2H), 6.75 (br s, 1H), 6.72 (br d, $J = 8.0$ Hz, 1H), 6.68 (br d, $J = 8.0$ Hz, 1H), 5.52 (br s, 1H), 2.30 (s, 3H), 1.16 (s, 9H); $^{13}\text{C}\{^1\text{H}\}$ NMR (125 MHz, CD_2Cl_2) δ (ppm) 151.0, 145.1, 139.5, 136.8, 136.0, 133.5, 130.3, 129.4, 128.1, 121.3, 120.9, 120.6, 116.9, 113.3, 26.7, 21.6, 19.7; Anal. Calcd for $\text{C}_{29}\text{H}_{31}\text{NOSi}$: C, 79.59; H, 7.14; N, 3.20, Found C, 79.41; H, 7.24; N, 3.37; HRMS-EI (m/z): calcd for $\text{C}_{29}\text{H}_{31}\text{NOSi}$ (M^+), 437.21749; found, 437.21606.

N-[4-(*tert*-Butyldiphenylsilyloxy)phenyl]-*N'*-phenyl-*N,N'*-di(*m*-tolyl)-biphenyl-4,4'-diamine (**9**)

8 (9.03 g, 20.6 mmol) and **3** (7.24 g, 17.5 mmol) were dissolved in dry toluene (50 mL). The solution was then transferred under a nitrogen atmosphere to a Schlenk tube containing $\text{Pd}_2(\text{dba})_3$ (0.28 g, 0.30 mmol) and DPPF (0.33 g, 0.60 mmol). Sodium *tert*-butoxide (4.18 g, 43.5 mmol) was then added and the mixture was heated to 100 °C. The solution was stirred under a nitrogen atmosphere for 23 h. The tube was then opened to air and toluene was evaporated under reduced pressure. The mixture was then dissolved in diethyl ether (100 mL), washed with water (2 × 200 mL), dried over magnesium sulfate and filtered. The solvent was evaporated under reduced pressure. The product was purified by column chromatography using hexane / toluene (4:1). Evaporating the solvent under reduced pressure yielded the desired product as a glassy solid (7.11 g, 53%). ^1H NMR (500 MHz, CD_2Cl_2) δ (ppm) 7.79 (d, $J = 6.6$ Hz, 4H), 7.52 – 7.41 (m, 10H), 7.31 (d, $J = 7.4$ Hz, 1H), 7.29 (d, $J = 7.4$ Hz, 1H), 7.20 (t, $J = 7.8$ Hz, 1H), 7.16 – 7.10 (m, 5H), 7.06 (t, $J = 7.3$ Hz, 1H), 7.02 (d, $J = 8.7$ Hz, 2H), 6.99 (br s, 1H), 6.94 (d, $J = 8.1$ Hz, 1H), 6.94 (d, $J = 8.1$ Hz, 1H), 6.92 (d, $J = 8.8$ Hz, 2H), 6.89 (br s, 1H), 6.85 (d, $J = 8.1$ Hz, 1H), 6.83 (d, $J = 7.6$ Hz, 1H), 6.77 (d, $J = 8.9$ Hz, 2H), 2.31 (s, 3H), 2.28 (s, 3H), 1.17 (s, 9H); $^{13}\text{C}\{^1\text{H}\}$ NMR (125 MHz, acetone- d_6) δ (ppm) 154.03, 149.72, 149.58, 149.07, 148.65, 143.05, 140.94, 140.70,

137.36, 136.44, 135.40, 134.61, 131.97, 131.17, 131.08, 130.90, 130.02, 129.73, 128.89, 128.82, 128.79, 126.84, 125.94, 125.81, 125.78, 125.71, 125.10, 124.67, 124.34, 123.45, 122.55, 122.37, 27.91, 22.45, 22.41, 20.95; Anal. Calcd for C₅₄H₅₀N₂OSi: C, 84.11; H, 6.54; N, 3.63, Found C, 83.97; H, 6.64; N, 3.56; HRMS-EI (*m/z*): calcd for C₅₄H₅₀N₂OSi (M⁺), 770.36924; found, 770.37509.

N-[4-(12-Bromododecyloxy)phenyl]-*N'*-phenyl-*N,N'*-di(*m*-tolyl)-biphenyl-4,4'-diamine (**10**)

1,12-Dibromododecane (8.5 g, 25.9 mmol) and **9** (2.0 g, 2.6 mmol) were placed together in a Schlenk ampule. The vessel was pump – filled three times. Dry, oxygen free THF (20 mL) was then added under nitrogen gas flow and the ampule was placed in an ice bath. Tetrabutylammonium fluoride (5.2 mL of a 1 M solution in THF) was added to the mixture. The reaction mixture was pumped down, sealed under static vacuum and stirred for 20 h at room temperature and additional 20 h at 50 °C. After that time the ampule was opened to air and the solvent was evaporated under reduced pressure. The product was purified by column chromatography using toluene / hexane (2:3) as eluent. Removing the solvent under reduced pressure gave the pure desired product as a glassy solid (0.96 g, 48%). ¹H NMR (500 MHz, acetone-*d*₆) δ (ppm) 7.55 (d, *J* = 8.6 Hz, 2H), 7.52 (d, *J* = 8.7 Hz, 2H), 7.27-7.32 (m, 2H), 7.13-7.22 (m, 2H), 6.99-7.09 (m, 9H), 6.81-6.95 (m, 8H), 3.99 (t, *J* = 6.4 Hz, 2H), 3.48 (t, *J* = 6.8 Hz, 2H), 2.25 (s, 3H), 2.24 (s, 3H), 1.85 (app. quint, *J* = 7.2 Hz, 2H), 1.78 (app. quint, *J* = 7.1 Hz, 2H), 1.28-1.53 (m, 16H); ¹³C{¹H} NMR (125 MHz, acetone-*d*₆) δ (ppm) 158.04, 149.90, 149.74, 149.60, 149.28, 148.65, 142.19, 140.96, 140.72, 136.51, 135.27, 131.18, 131.08, 130.91, 129.31, 128.89, 128.83, 126.84, 125.94, 125.82, 125.74, 125.66, 124.99, 124.68, 124.21, 123.45, 122.28,

117.28, 69.75, 35.81, 34.62, 31.07, 30.44, 29.79, 27.79, 22.47, 22.41;[†] Anal. Calcd for C₅₀H₅₅BrN₂O: C, 77.00; H, 7.11; N, 3.59, Found C, 77.08; H, 7.15; N, 3.60; HRMS-EI (*m/z*): calcd for C₅₀H₅₅BrN₂O (M⁺), 778.34978; found, 778.34884.

N-[4-(12-Mercaptododecyloxy)phenyl]-*N'*-phenyl-*N,N'*-di(*m*-tolyl)-biphenyl-4,4'-diamine (**TPD-C12-thiol**)

10 (0.90 g, 1.2 mmol) and thiourea (0.30 g, 3.9 mmol) were placed together into a Schlenk ampule. DMF (15 mL) was added and the mixture was deoxygenated by bubbling with nitrogen gas for 30 min followed by pump-filling the vessel three times. The mixture was sealed under static vacuum and stirred at 100 °C for 20 h. TLC analysis revealed that the starting bromide was consumed and was consistent with the formation of the corresponding thiuronium salt. The hydrolysis of the salt was performed as follows. Potassium hydroxide (1.96 g, 35.0 mmol) was dissolved in water (10 mL). The solution was bubbled with nitrogen gas for 40 min. The hydroxide solution was then transferred to the reaction mixture under inert atmosphere. The reaction mixture was brought back to static vacuum and stirred at 100 °C for 20 h. The ampule was then placed in an ice bath and it was opened to nitrogen gas flow. 1 M HCl was added to the mixture until pH reached ca. 5 and the product was extracted with dichloromethane (100 mL). The organic phase was washed with water (3 × 100 mL), dried over sodium sulfate and filtered. The solvent was removed under reduced pressure. The product was purified by column chromatography using toluene / hexane mixture (1:1) as eluent. After removing the solvent under reduced pressure the pure desired product was collected (0.58 g, 69%). ¹H NMR (500 MHz, acetone-*d*₆) δ (ppm) 7.52 (d, *J* = 8.7 Hz, 2H), 7.50 (d, *J* = 8.8 Hz, 2H), 7.26-7.30 (m, 2H), 7.18 (t, *J* = 7.8 Hz, 1H), 7.14 (t, *J* = 7.8 Hz, 1H), 7.02-7.07 (m, 6H), 7.00 (d, *J* = 8.7 Hz, 2H), 6.79-6.93

[†] Five aliphatic carbon signals are missing most likely due to an overlap.

(m, 9H), 3.98 (t, $J = 6.5$ Hz, 2H), 2.49 (app. q, $J = 7.4$, 2H), 2.24 (s, 3H), 2.22 (s, 3H), 1.77 (app. quint, $J = 7.1$ Hz, 2H), 1.63 (t, $J = 7.8$ Hz, 1H), 1.58 (app. quint, $J = 7.4$ Hz, 2H), 1.48 (app. quint, $J = 7.3$ Hz, 2H), 1.25-1.41 (m, 14H); $^{13}\text{C}\{^1\text{H}\}$ NMR (125 MHz, CDCl_3) δ (ppm) 157.96, 149.85, 149.68, 149.55, 149.22, 148.59, 142.15, 140.92, 140.68, 136.43, 135.20, 131.15, 131.06, 130.89, 129.26, 128.85, 128.79, 126.79, 125.90, 125.78, 125.71, 125.62, 124.96, 124.66, 124.18, 123.40, 122.24, 117.25, 69.73, 35.82, 31.26, 31.23, 31.06, 31.03, 30.77, 29.99, 27.76, 25.79, 22.46, 22.40;[‡] Anal. Calcd for $\text{C}_{50}\text{H}_{56}\text{N}_2\text{OS}$: C, 81.92; H, 7.70; N, 3.82, Found C, 81.85; H, 7.78; N, 3.82; HRMS-EI (m/z): calcd for $\text{C}_{50}\text{H}_{56}\text{N}_2\text{OS}$ (M^+), 732.41134; found, 732.40701.

N-[4-(dodecyloxy)phenyl]-*N'*-phenyl-*N,N'*-di(*m*-tolyl)-biphenyl-4,4'-diamine (**C12-TPD**)

1-Bromododecane (1.25 g, 5.0 mmol) and **9** (1.00 g, 1.3 mmol) were placed together in a Schlenk ampule. The vessel was pump – filled three times. Dry, oxygen free THF (8 mL) was then added under nitrogen gas flow. The ampule was placed in an ice bath and tetrabutylammonium fluoride (3 mL of a 1 M solution in THF) was added to the mixture. The reaction mixture was pumped down, sealed under static vacuum and stirred for 20 h at 60 °C. The solvent was then evaporated under reduced pressure and the crude product was loaded onto a short silica plug. The unreacted bromide was washed off with hexanes. This was followed by a wash with hexanes / toluene mixture (1:1), which eluted the desired product. Removing the solvent under reduced pressure yielded the product as a glassy solid (0.71 g, 78%). ^1H NMR (500 MHz, acetone- d_6) δ (ppm) 7.55 (d, $J = 8.6$ Hz, 2H), 7.52 (d, $J = 8.7$ Hz, 2H), 7.26-7.32 (m, 2H), 7.12-7.22 (m, 2H), 6.98-7.09 (m, 9H), 6.80-6.95 (m, 8H), 4.00 (t, $J = 6.3$ Hz, 2H), 2.25 (s, 3H), 2.24 (s, 3H), 1.78 (app. quint, $J = 6.9$ Hz, 2H), 1.45-1.53 (m, 2H), 1.21-1.42 (m, 16H), 0.87 (app. t, $J = 6.9$ Hz, 3H); $^{13}\text{C}\{^1\text{H}\}$ NMR

[‡] Two aliphatic carbon signals are missing most likely due to an overlap.

(125 MHz, acetone-*d*₆) δ (ppm) 158.04, 149.91, 149.74, 149.60, 149.29, 148.65, 142.19, 140.96, 140.72, 136.51, 135.27, 131.18, 131.09, 130.92, 129.31, 128.89, 128.83, 126.84, 125.94, 125.82, 125.74, 125.67, 124.99, 124.68, 124.21, 123.45, 122.29, 117.28, 69.76, 33.63, 31.38, 31.35, 31.33, 27.80, 24.32, 22.47, 22.41, 15.35;[§] Anal. Calcd for C₅₀H₅₆N₂O: C, 85.67; H, 8.05; N, 4.00, Found C, 85.61; H, 8.06; N, 3.99; HRMS-EI (*m/z*): calcd for C₅₀H₅₆N₂O (M⁺), 700.43926; found, 700.43933.

Chemical Oxidation of C12-TPD in Solution

A dry dichloromethane solution of a substoichiometric amount of [(*p*-BrC₆H₄)₃N]^{•+} [SbCl₆]⁻ was added to a dry toluene solution of **C12-TPD**. The absorption spectrum of the solution in the UV-Vis-NIR range was acquired in a 1 cm cuvette.

Preparation of Oleylamine-coated Au NPs

Hydrogen tetrachloroaurate (III) trihydrate (0.66 g, 1.68 mmol) was dissolved in a mixture of toluene (6 mL) and freshly distilled oleylamine, OA (6 mL, Acros). The solution was then added into a mixture of toluene (50 mL) and oleylamine (12 mL). While the mixture was stirred at room temperature methanol (6 mL) was added. Sodium borohydride (0.12 g, 3.2 mmol) was then added at once to the stirred solution resulting in an immediate appearance of a dark color. The mixture was stirred for additional 2 h and was then poured into acetonitrile (100 mL). The precipitate that formed was washed twice with acetonitrile and twice with methanol. The procedure yielded nanoparticles (0.32 g) with size distribution of particle diameters 3 ± 1.1 nm, as estimated from TEM analysis.

[§] Four aliphatic carbon signals are missing most likely due to an overlap.

General Procedure for Reacting OA-Coated Gold Nanoparticles with Thiols

A known amount of OA-coated gold nanoparticles was dissolved in toluene (concentration ca. 15 mg/mL). Next, the thiol of choice (dodecanethiol, **TPD-Cx-thiol** with $x = 3$ or 12) or mixture of **TPD-Cx-thiol** and dodecanethiol (with 60% of dodecanethiol by mole in the mixture of two thiols) was added at once in twofold excess, and the mixture was stirred in the dark for 20 h.** Then the particles were precipitated with addition of methanol and the resulting precipitate was washed with a methanol / toluene mixture (1:1) until no fluorescence was observed in the supernatant. All of the syntheses described here were done on a 15–20 mg scale.

TEM Analysis

A toluene solution of each NP sample was drop casted onto a holey carbon-coated copper grid substrate. The analysis was performed using a JEOL 100 CX-II system at 100 kV acceleration voltage. The instrument is equipped with a calibrated CCD camera that was used to acquire the images. More than 400 particles were analyzed for each sample using the freeware ImageJ to obtain particle size distribution. The histograms of diameters of the prepared nanoparticles as well as their average diameters with the corresponding standard deviations are shown in Figure S3. As can be seen from the figure the distributions of sizes were rather similar for all of the analyzed samples and the standard deviations from the average particle diameters

** The stoichiometry of the reaction was calculated assuming the thiol footprint (F_{thiol}) of 22 \AA^2 (based on Schreiber, F. *Prog. Surf. Sci.* **2000**, *65*, 151-257) and the total mass of starting NPs (m_{NP}) coming from metallic gold with density $d_{Au} = 19.3 \text{ g/cm}^3$. The total surface of particles (S) is then given by $S = \frac{3m_{NP}}{rd_{Au}}$, where r is particle radius (1.5 nm). The needed amount of moles of the thiol (n_{thiol}) was calculated according to $n_{thiol} = \frac{S}{N_A F_{thiol}}$.

were around 30% for most of the samples. These data show that the employed synthetic procedure generated nanoparticles that were characterized by rather similar size distributions, independently of the specific **TPD-Cx-thiol** used in the synthesis.

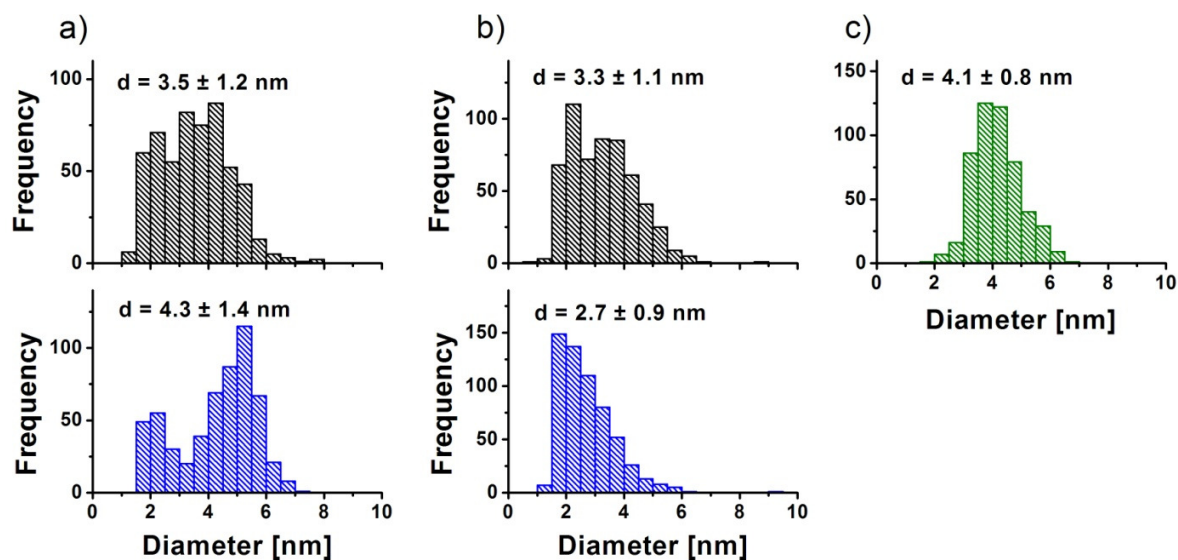


Fig. S3 Histograms and calculated average values and standard deviation of particle diameters measured for a) **AuS-C3-TPD** (top graph, black color) and the corresponding mixed monolayer system **AuS-C3-TPD(DDT₆₀)** (bottom graph, blue color); b) **AuS-C12-TPD** (top graph, black color) and the corresponding mixed monolayer system **AuS-C12-TPD(DDT₆₀)** (bottom graph, blue color); c) Au NPs coated with dodecanethiol (**AuS-C12**).

FT-IR Analysis of Mixed-ligand Au NPs

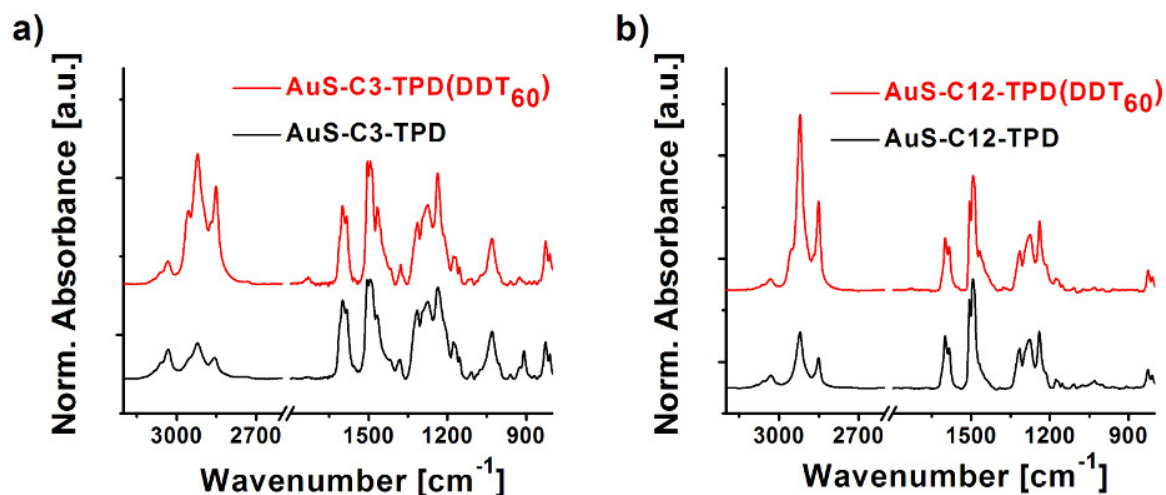


Fig. S4 FT-IR spectra of neat films of Au NP samples coated with mixtures of a) **TPD-C3-thiol** and dodecanethiol and b) **TPD-C12-thiol** and dodecanethiol. The spectra of the corresponding Au NP containing only the TPD ligands are included for comparison. All spectra were normalized at 1600 cm^{-1} and displaced vertically for clarity.

It is clear from the graphs in Figure S4 that the signal in the spectral region of alkyl C-H stretching modes ($2800 - 3000\text{ cm}^{-1}$) is significantly higher for the samples prepared in the presence of mixtures of **TPD-Cx-thiol** and dodecanethiol than for the NPs prepared with **TPD-Cx-thiols** only, when the spectra are normalized to a mode originating from the TPD moiety. This is consistent with incorporating dodecanethiol into the NP samples and supports the presence of two types of ligands on the surface of Au NPs that were prepared using mixtures of **TPD-Cx-thiol** and dodecanethiol.

Calculations of Residual Oleylamine in AuS-C3-TPD and AuS-C12-TPD Based on ^1H NMR Measurements

Method I

A spectrum was divided into two parts: an aliphatic part (0.0 – 4.5 ppm) and the spectral region characteristic for protons attached to unsaturated carbon atoms (4.5 – 8.0 ppm), and the total integrated signal in each part (not including signals from water and residual solvent) was measured, I_{aliph} and I_{unsat} . If a mixture of **TPD-Cx-thiol** and OA are present in the NP sample, the total signals expected for the aliphatic protons and the protons attached to unsaturated carbon atoms are given by equations *a* and *b*, respectively:

$$a) \quad I_{aliph} = (2x + 6)[\text{TPD-Cx-thiol}]_{\%} + 35[\text{OA}]_{\%}$$

$$b) \quad I_{unsat} = 25[\text{TPD-Cx-thiol}]_{\%} + 2[\text{OA}]_{\%}$$

For each type of NPs ($x = 3, 12$), the equations above can be solved for the two unknown percentage values $[\text{TPD-Cx-thiol}]_{\%}$ and $[\text{OA}]_{\%}$. The following values were obtained: $[\text{TPD-C3-thiol}]_{\%} = 88\%$, $[\text{TPD-C12-thiol}]_{\%} = 100\%$.

Method II

Since neither **TPD-C3-thiol** nor **TPD-C12-thiol** has a methyl group attached to an alkyl chain the integrated signal from such methyl groups (around 0.9 ppm), I_{methyl} , can be attributed to the methyl group from residual oleylamine (Eq. *c*). The total integrated signal I_{total} can be expressed by Eq. *d*:

$$c) \quad I_{methyl} = 3[\text{OA}]_{\%}$$

$$d) \quad I_{total} = (31 + 2x)[\text{TPD-Cx-thiol}]_{\%} + 37[\text{OA}]_{\%}$$

Again, for each NP sample, equations *c-d* can be solved for the two unknown percentage values [TPD-Cx-thiol]_% and [OA]_%, using the experimental values for the integrations of I_{methyl} and I_{total} . The calculated values were [TPD-C3-thiol]_% = 95% and [TPD-C12-thiol]_% = 98%.

The results from the two methods for each sample were averaged, yielding: [TPD-C3-thiol]_% = 92% and [TPD-C12-thiol]_% = 99%. Thus we can conclude that the amount of residual oleylamine is below 10% in both **AuS-C3-TPD** and **AuS-C12-TPD**.

Calculation of the Average Dye-dye Distance Ratio for AuS-C3-TPD and AuS-C12-TPD

Assuming the same molecular footprint and fully extended alkyl spacers in both **AuS-C3-TPD** and **AuS-C12-TPD**, we calculated the ratio of average dye-dye distances for the two systems according to $\frac{D_{AuS-C12-TPD}}{D_{AuS-C3-TPD}} = \frac{r_{Au\ NP} + d_{C12}}{r_{Au\ NP} + d_{C3}}$, where $D_{AuS-Cx-TPD}$ is the average dye-dye distance in the **AuS-Cx-TPD** system, and $r_{Au\ NP} + d_{Cx}$ is the sum of the NP radius ($r_{Au\ NP}$, here 1.7 nm) and the length of the a fully extended alkyl spacer (d_{Cx} , 0.5 nm and 1.6 nm for C3 and C12 linkers, respectively).

UV-Vis Absorption Spectra and Analysis of the Mixed-ligand Au NP Systems

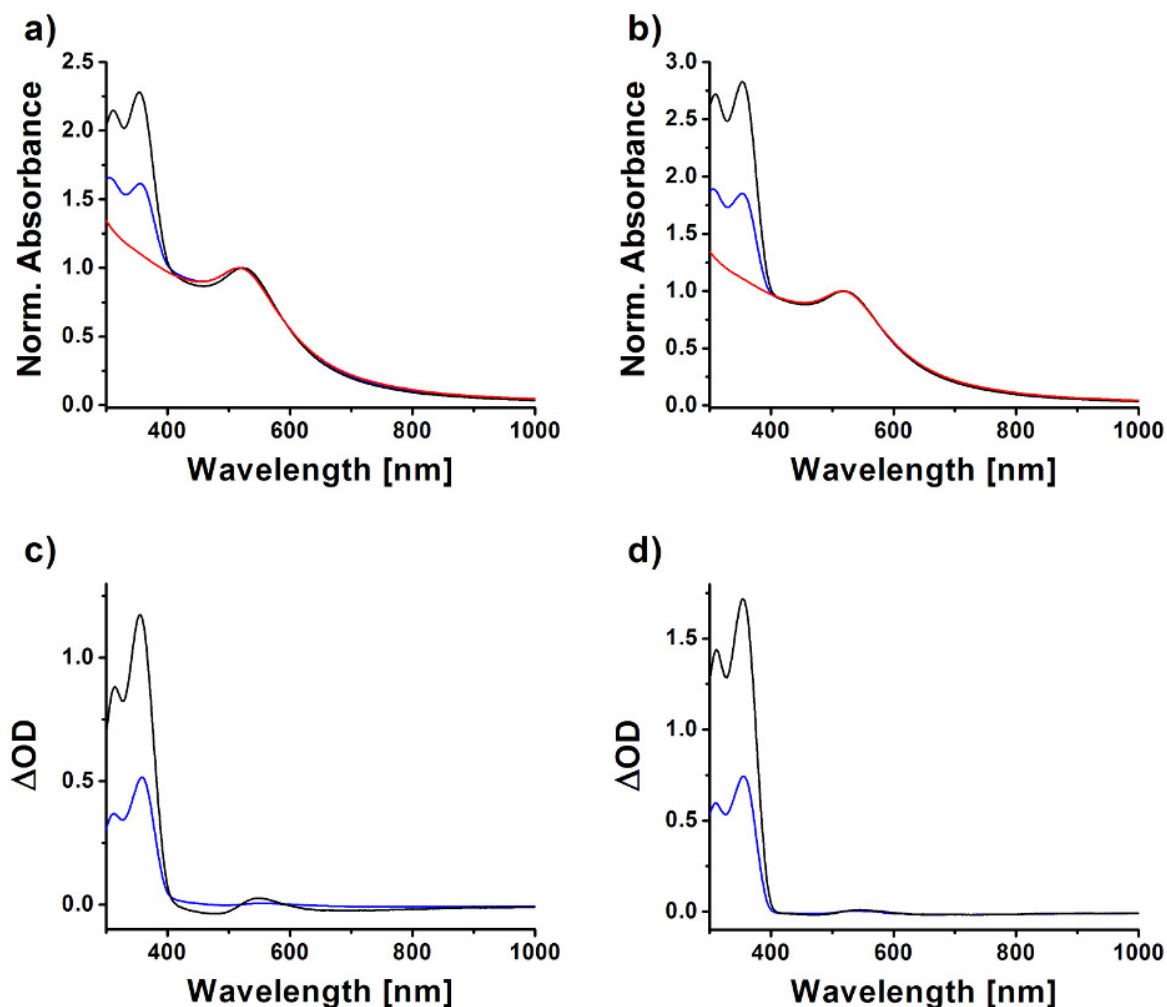


Fig. S5 Top panel: normalized absorption spectra of toluene solutions of a) **AuS-C3-TPD** (black line), the corresponding mixed monolayer system **AuS-C3-TPD(DDT₆₀)** (blue line), and **AuS-C12** (red line); b) **AuS-C12-TPD** (black line), the corresponding mixed monolayer system **AuS-C12-TPD(DDT₆₀)** (blue line), and **AuS-C12** (red line); all spectra were normalized at the plasmon resonance band maximum around 520 nm. Bottom panel: residual optical density after subtracting the normalized spectrum of **AuS-C12** from c) **AuS-C3-TPD** (black line), and **AuS-**

C3-TPD(DDT₆₀) (blue line); d) **AuS-C12-TPD** (black line), and **AuS-C12-TPD(DDT₆₀)** (blue line).

Assuming the molar extinction coefficient of the TPD moiety is the same in both high-TPD-coverage and mixed-monolayer systems, the values of absorbance due to the TPD moiety (band around 350 nm) can be used to estimate the fraction of TPD ligands present in the mixed monolayer systems (after subtraction of the contribution from the metal core, Figure S5c and S5d). The calculated values were 44% and 43% for the **AuS-C3-TPD(DDT₆₀)** mixed monolayer system and the **AuS-C12-TPD(DDT₆₀)** mixed monolayer system, respectively.

Time-Correlated Single Photon Counting Measurements

Fluorescence lifetimes of solutions were measured using the time-correlated single-photon counting technique. A schematic representation of the optical setup is shown in Figure S6. A femtosecond mode-locked Ti:Sapphire laser (Tsunami, Spectra-Physics) pumped by a 5W diode laser (Millennia, Spectra-Physics) was used as the excitation source. The laser generated pulses of mean power ~0.5 W with a repetition rate of ~81 MHz at 730 nm. A small fraction of the laser beam light was directed to a spectrum analyzer by beam splitter BS2. The rest of the beam was split (BS1) and ca. 5% of the beam was focused onto the timing photodiode (Newport 818-BB-21A, PD1). The photodiode signal was used to drive a constant-fraction discriminator (Tennelec TC455 Quad, CFD2). The rate of the discriminator output pulses was reduced sixteen times with the use of a frequency divider (Pulse Research Lab, PRL-256N, FD). The divided signal was sent through another constant fraction discriminator (CFD4) to the stop input of a time-to-amplitude converter (Ortec 457, TAC). The majority of the laser beam was focused onto

a BBO crystal and frequency doubled. The resulting second harmonic (365 nm) and the fundamental beams were separated after passing a quartz prism and a half-wave plate. The fundamental beam was blocked and the frequency-doubled beam was sent through a pinhole to a Glan-Thompson polarizer (POL1) with the transmitted polarization direction oriented perpendicularly to the surface of the table. The power at the sample was controlled by rotating the polarization plane of the half-wave plate. The beam was passed through a beam splitter (BS3) and the reflected light was focused onto a DC-coupled photodiode (Thorlabs DET210, PD2) connected to a series RC circuit with a time constant of 0.22 sec. The output of the RC circuit was connected to an input of a DAQ board (National Instruments, USB-6221 BNC) connected via a USB port to a PC. This electronic setup was used as the “signal integrator”, effectively measuring the relative energy dose at the sample. The beam transmitted by BS3 was focused on the sample by a quartz lens with a 30 cm focal length. The sample holder was masked so only a small portion of the fluorescence light was collected. The fluorescence was detected at 90° with respect to the excitation beam. The fluorescence light was collimated by a quartz lens and sent through a sheet polarizer (POL2) with its polarization plane rotated by the magic angle (54.7°) to the normal of the surface of the table. The light was then sent through a depolarizer (DEPOL) and focused onto the entrance slit of a monochromator (Instruments SA H10, 1200 grooves/mm, 100 mm path length, Mono). The monochromatic light was then sent to a photomultiplier tube (Hamamatsu R1564U-01, PMT) biased at 3250 V. The pulses from the photomultiplier were amplified by a 1 GHz amplifier (Ortec 9306, Amp) and sent to a constant fraction discriminator (CFD3) and then to the start input of the TAC. The output of the TAC was directed to a pulse height analyzer (Ortec-Norland 5600 Multichannel Analyzer, PHA), and transferred to a personal computer (PC). The PHA channel width was determined for each experiment from the distance between two consecutive input laser pulses and the repetition rate of the laser (measured by the

timing photodiode PD2 and a pulse counter (Protek B-808)). The Instrument Response Function (IRF) was measured before each decay experiment using silica particles suspended in water (Ludox, Aldrich). The FWHM of the response function was between 50 and 70 ps. The system was optimized by checking the goodness of the fit (χ^2 , randomness of residual function) and the extracted value of the fluorescence lifetime of the fitted decay function of 1,4-bis(5-phenyloxazol-2-yl) benzene (POPOP) in degassed cyclohexane.^{3,4} Generally values of χ^2 lower than 1.20 indicated good fits. In order to ensure operation in the linear regime of the electronics, the count rate at the Start input of TAC was kept below 10 kcps. The concentrations of solutions were such that the ΔOD in a 1 cm cuvette was not larger than 0.05 (ca. 1 μM for **C12-TPD** toluene solution). Both IRFs and decays were collected until the number of counts at the maximum reached 10,000, although for the unstable NP sample only 2,000 counts at the maximum were collected. The experimental data were fitted using the free CFS_LS software.^{††}

^{††} <http://cfs.umbi.umd.edu/cfs/software/index.html>

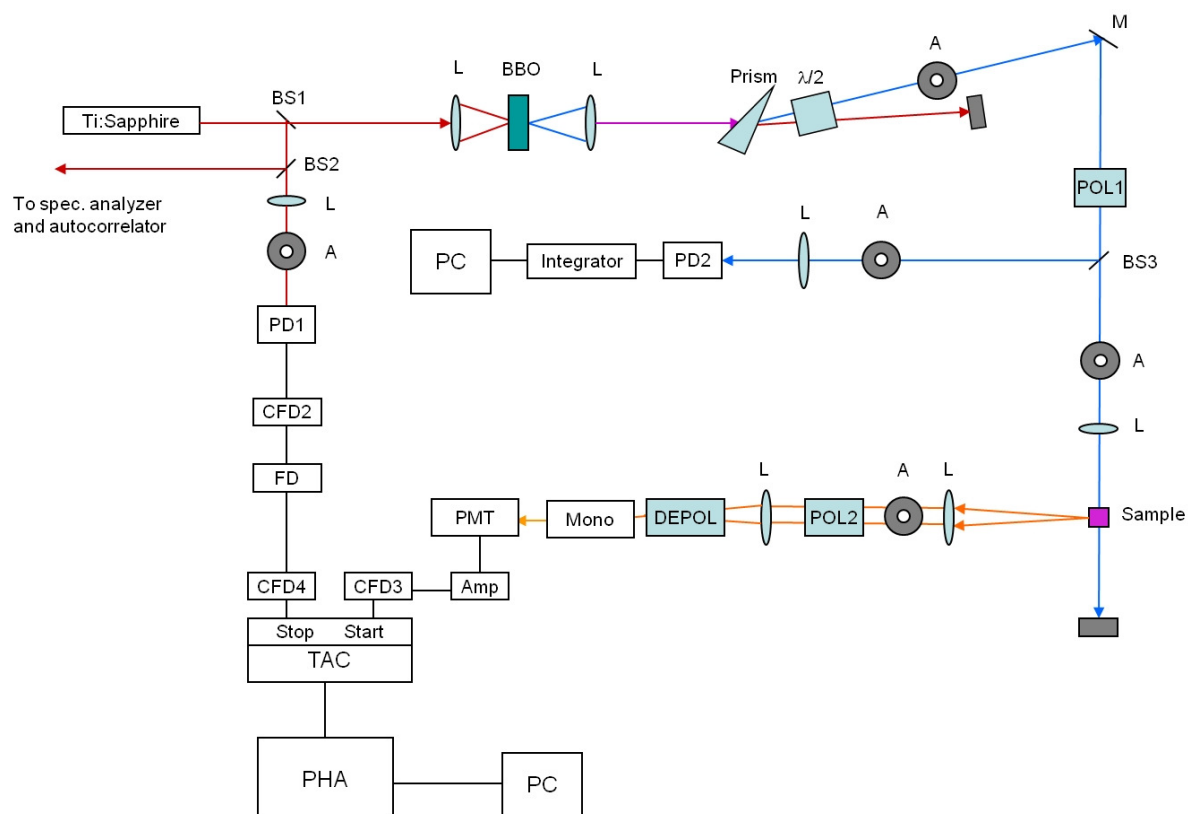


Fig. S6 Scheme of the optical layout of the TC-SPC experiment; L = lens, A = aperture, $\lambda/2$ = Half-wave plate. See text for details.

Analysis of the TC-SPC data acquired for AuS-C12-TPD

Figure S7a shows the fluorescence decay measured for a toluene solution of **AuS-C12-TPD** (A, black circles). There is an obvious contribution from at least two components to the decay: one very fast and one with a much longer lifetime. Tail fitting of the data with a monoexponential decay function resulted in the lifetime of ca. 960 ps for the slow component. A monoexponential decay test function with the lifetime of 960 ps was then convoluted with the instrument response function (IRF) and multiplied by a synthesized Poissonian noise with the use of the CFS_LS software. The simulated decay function was then multiplied by a factor such that the intensity of the resulting function matched the intensity of the measured decay in the tail

region. This resulted in the simulated decay (B) represented by the red circles in Figure S7a. The simulated decay was then subtracted from the measured decay (A - B) yielding the profile of the short-lived component. As can be seen in Figure S7b the shape of the fast component (A - B in Figure S7a) is practically the same as the shape of the IRF, implying that the decay rate of the fast component is too fast to be resolved with the TC-SPC setup. The numerically integrated signal of the short-lived component (A - B in Figure S7A) was found to be ca. 25% of the total integrated signal of the measured decay (A in Figure S7a).

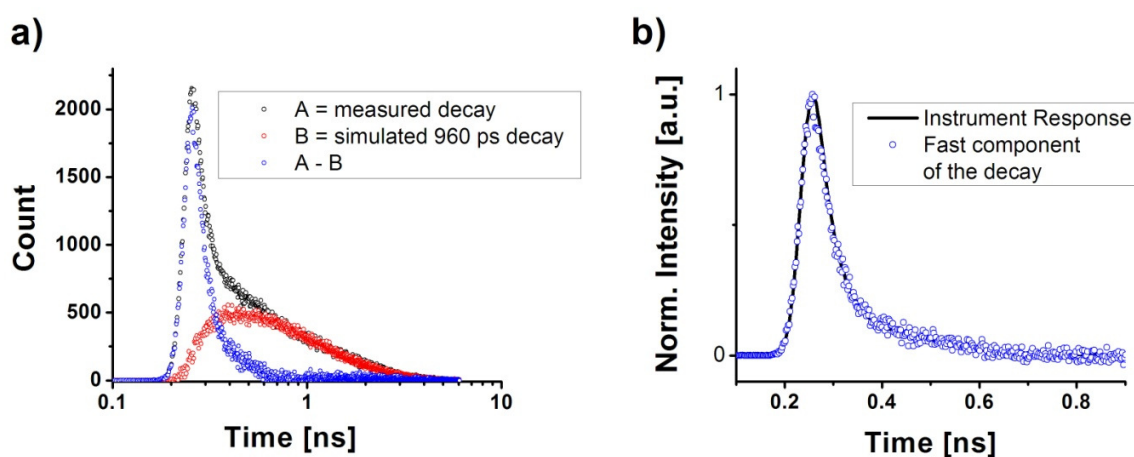


Fig. S7 a) Analysis of the fluorescence decay measured for a toluene solution of **AuS-C12-TPD**, b) comparison of the instrument response function with the fast decay component present in the acquired data.

Based on the excited-state lifetime of TPD moieties attached to Au NPs in **AuS-C12-TPD** measured with the use of fs transient absorption method (ca. 2.4 ps, see Figure 8d) and on the known lifetime of the long-lived signal (ca. 960 ps), the fluorescence decay measured for the toluene solution of **AuS-C12-TPD** was fitted with the following function convoluted with the IRF:

$$I(t) = A_1 e^{-\frac{t}{2.4 \text{ ps}}} + A_2 e^{-\frac{t}{960 \text{ ps}}},$$

where $I(t)$ is the signal intensity. The best fit (defined as the fit with the lowest value of χ^2 which in this case was found to be 1.12) was found for the preexponential amplitudes $A_1 = 56$ (99%) and $A_2 = 0.6$ (1%). The preexponential amplitudes in the decay function are proportional to the number of photoexcited molecules from which the fluorescence signals originate. Based on the values of A_1 and A_2 it can be concluded that the number of molecules exhibiting the long-lived fluorescence signal (960 ps lifetime, B in Figure S7a) constitutes only ca. 1% of the photoexcited TPD moieties and a vast majority of molecules (99%) exhibit a very short fluorescence lifetime (A - B in Figure S7a), consistent with the fs TA measurements.

Femtosecond Transient Absorption Measurements

Although the transient kinetic signal response for metallic NPs can be quite strong in the spectral region close to that of the surface-plasmon absorption band,^{5, 6} the contribution of the metal core to the transient signal can be relatively small when the spectral separation between the Au NP surface-plasmon band (ca. 520 nm) and the probe wavelength is large. This is the case for the experiments carried out in this work, where the samples were probed in the NIR range (850 – 1650 nm). Nonetheless, for completeness, the contribution to the overall transient signal from the metal NP was appropriately subtracted, as detailed in the following, before any further data processing. Figure S8 shows a few transient spectra measured for a toluene solution of **AuS-C12**. Since in this sample the metallic core is the only species giving rise to the measured signal, the gathered data can be used to subtract the contribution of the Au NP core to the ΔOD in the other NP samples. The subtraction was performed under the following assumptions. Firstly, the ground-state absorption cross sections at the excitation wavelength (350 nm) of both the metallic

core (σ_{Au}) and the TPD moiety (σ_{TPD}) were assumed to be the same from sample to sample. We used $\sigma_{Au} = 6.3 \times 10^{-15} \text{ cm}^2/\text{particle}$, which is a value based on a literature report on the molar extinction coefficient established for Au NPs (diameter ca. 3 nm) in toluene solutions.⁷ The value of $\sigma_{TPD} = 1.5 \times 10^{-16} \text{ cm}^2/\text{molecule}$ was obtained from the molar extinction coefficient at 350 nm established from absorption measurements of a series of toluene solutions of **C12-TPD** of known concentration ($\epsilon_{C12-TPD} = 3.97 \times 10^4 \text{ Lmol}^{-1}\text{cm}^{-1}$). Secondly, the decay dynamics of the excited state of the metallic core was assumed to be the same for each NP sample. The third assumption was that the excited states of the Au NP metallic core and of the TPD moiety each have negligible absorption cross sections at 350 nm.

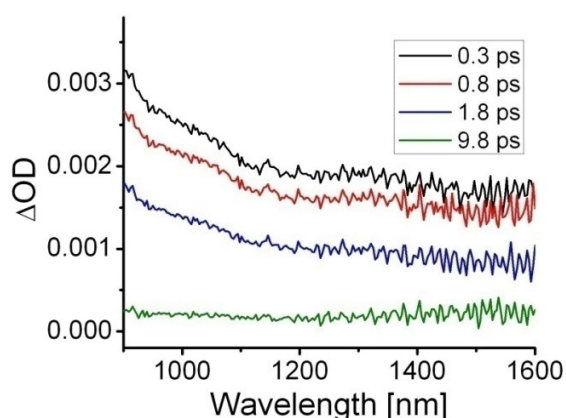


Fig. S8. Transient spectra measured for a toluene solution of **AuS-C12**. The delay values are shown in the legend.

In order to subtract the contribution from the metallic core of Au NPs from the measured ΔOD signal, the excited-state populations of Au NPs in **AuS-C12** and in the samples containing TPD moieties were calculated as follows. The propagation of the excitation beam with photon

fluence $\Phi_0 = 7.2 \times 10^{14}$ photons/cm² at the front face of the sample^{‡‡} was modeled through the 2 mm path length of a sample containing known concentrations of Au NP metallic cores and TPD moieties (as estimated from the absorbance of the samples), describing the system as a series of thin slabs with planes perpendicular to the direction of beam propagation.^{§§} Excitation beam attenuation and ground-state population depletion of both the metallic core and the TPD moiety in each slab were computed according to the following equations and then used as input for the following slab:

- $\Phi_n = \Phi_{n-1} e^{-[(N_{Au}^0 - N_{Au}^{*n})\sigma_{Au} + (N_{TPD}^0 - N_{TPD}^{*n})\sigma_{TPD}]\Delta l}$,
- $N_{Au}^{*n} = N_{Au}^0 (1 - e^{-\sigma_{Au}\Phi_n})$,
- $N_{TPD}^{*n} = N_{TPD}^0 (1 - e^{-\sigma_{TPD}\Phi_n})$,

where Φ_n , Φ_{n-1} are the excitation beam fluence values at the n 'th slab and in the slab immediately before respectively, N_{Au}^0 , N_{TPD}^0 are the ground-state populations of the Au NP metallic core and the TPD moiety respectively, N_{Au}^{*n} , N_{TPD}^{*n} are the excited-state populations of the Au NP metallic core and the TPD moiety in the n 'th slab respectively, σ_{Au} , σ_{TPD} are the ground-state cross sections at 350 nm for the Au NP metallic core and the TPD moiety respectively, and Δl is the path length of the slab. Such computation was repeated for each slab until the end of the

^{‡‡} The fluence was calculated using the measured power of the excitation (pump) beam at the front face of the sample (2.1 mW), repetition rate of the laser (1 kHz), the photon energy (5.7×10^{-19} J), and the overlap of the pump and probe beams, both of which were measured to have a gaussian spatial distribution with parameters $\sigma_{pump} = 310 \mu\text{m}$ (HW1/e) and $\sigma_{probe} = 170 \mu\text{m}$ (HW1/e). Only overlap in the circular area with the radius of $2\sigma_{probe}$ was taken into account for fluence calculations. For further calculations the intensity profiles of the overlapped beams were assumed to be constant over the overlap region.

^{§§} This approach was taken in order to account for both the ground-state depletion of the two-component system (TPD moiety and Au NP metallic core) and the excitation beam attenuation through the sample as the studied solutions had high absorbance values at the excitation wavelength.

path length was reached ($n = 5000$).^{***} The output of the calculation was the value of fluence of the excitation beam after passing through the sample, and the total initial excited-state populations of both the Au NP metallic core ($N_{Au}^* = \sum_{n=0}^{5000} N_{Au}^{*n}$) and the TPD moiety ($N_{TPD}^* = \sum_{n=0}^{5000} N_{TPD}^{*n}$).^{†††}

The kinetic profiles of ΔOD measured at different wavelengths for **AuS-C12** were then multiplied by a factor $\frac{N_{Au}^{S*}}{N_{Au}^{ref*}}$, where N_{Au}^{S*} and N_{Au}^{ref*} are the total initial excited-state populations of Au NP metallic core calculated as discussed above for the sample of interest and the **AuS-C12** reference, respectively. The scaled kinetic traces of **AuS-C12** were then subtracted from the kinetic traces of the sample of interest, thus removing the contribution of Au NP metallic core to the measured ΔOD . Figure S9 shows an example of the kinetic traces measured for **AuS-C12-TPD** at a few wavelengths before and after subtraction of the scaled traces of **AuS-C12**.

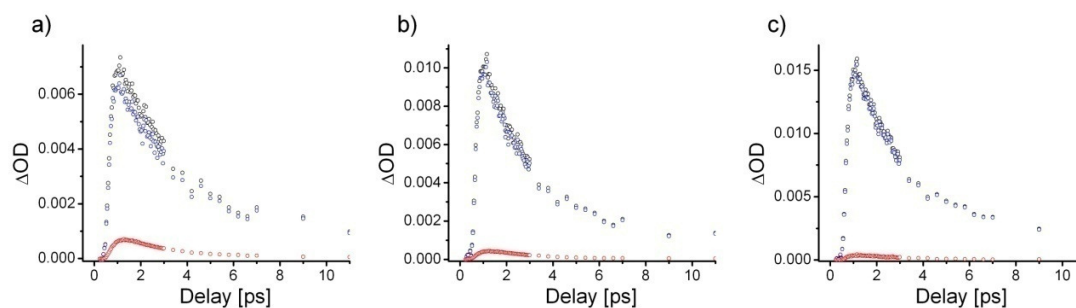


Fig. S9. Kinetic traces before (black circles) and after (blue circles) subtraction of the scaled trace of **AuS-C12** (red circles) from traces measured for **AuS-C12-TPD** at a) 900 nm, b) 1200 nm, and c) 1600 nm.

^{***} We found that a change in the number of slabs above 4000 had negligible effect on the output values.

^{†††} In all the samples, the calculated fraction of photoexcited TPD moiety population was less than 10% of the total population.

Femtosecond transient absorption data fitting procedure

The kinetic traces at different wavelengths treated as described above were analyzed using a global fitting routine where the fitting function was a sum of exponential functions of the form:

$\Delta OD = A_1 e^{-\frac{t}{\tau_1}} + A_2 e^{-\frac{t}{\tau_2}} + \dots + y_0$, where t is the variable temporal delay of each data point, A_1 , A_2 , ... are the preexponential amplitudes, τ_1 , τ_2 , ... are the decay lifetimes, and y_0 is a time-independent offset. This was implemented in the Origin 7.5 software. The only global parameters used in the fitting routine were the decay lifetimes. The fitting routine returned these constants as well as a corresponding set of preexponential amplitudes and offset for each wavelength.

Femtosecond transient absorption supporting data

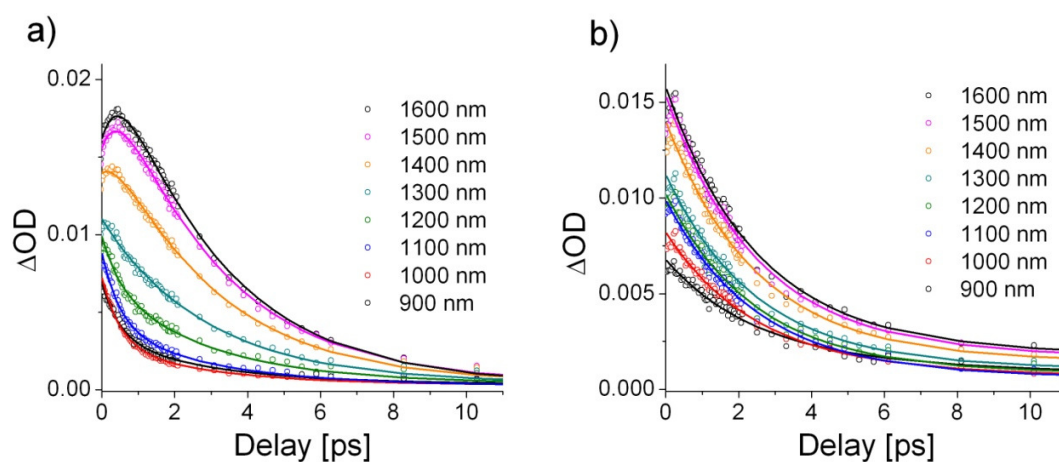


Fig. S10 Kinetic traces at different wavelengths (circles) and the corresponding curves from data fitting with a sum of two exponential functions (solid lines) for a) **AuS-C3-TPD** and b) **AuS-C12-TPD**. The corresponding lifetimes and preexponential amplitudes from the fitting for these samples are shown in Fig. 8b&d of the paper.

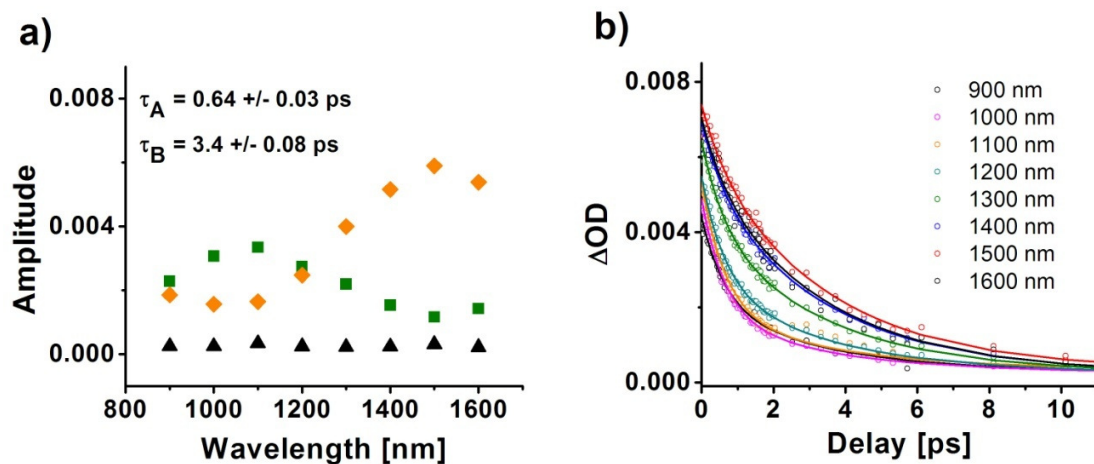


Fig. S11 a) Lifetimes and spectral distribution of preexponential amplitudes (\blacksquare for τ_A , \blacklozenge for τ_B , \blacktriangle for offset) obtained from global fitting (with a sum of two exponential decays) of the data acquired for a toluene solution of AuS-C3-TPD(DDT₆₀); b) kinetic traces (circles) and the corresponding curves from fitting the data (solid lines) with a sum of two exponential functions for the same sample as in a).

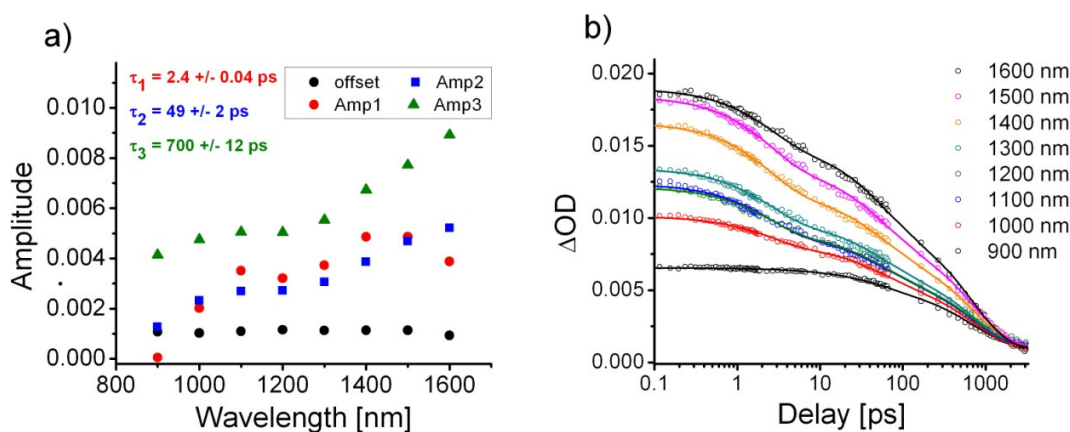


Fig. S12 a) Lifetimes and spectral distribution of preexponential amplitudes obtained by fitting the data for a C12-TPD 0.1 M toluene solution with a sum of three exponential functions; b) kinetic traces (circles) and the corresponding curves from fitting the data (solid lines) with a sum of three exponential functions for the same sample as in a). The discrepancy between the lifetime of the singlet excited state of C12-TPD assigned here to $\tau_3 = 700 \pm 12$ ps and the fluorescence lifetime obtained from the time-

correlated single-photon counting technique ($\tau = 0.98$ ns) most likely originates from the difference in concentration between the 1 μ M solution analyzed with TC-SPC and the 0.1 M solution examined with the fs TA technique, i.e., concentration quenching effects shorten the excited state lifetime in the 0.1 M solution.

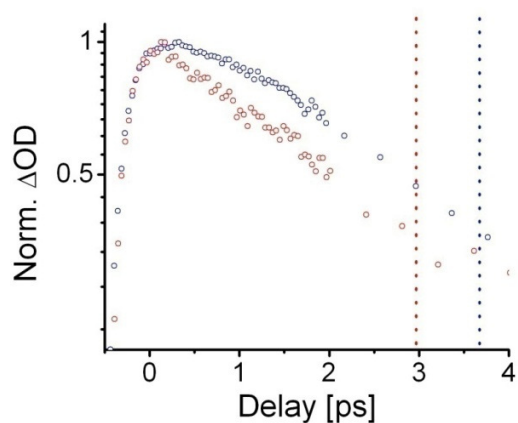


Fig. S13 Normalized kinetic traces measured at 1600 nm for **AuS-C12-TPD** (red circles) and **AuS-C3-TPD** (blue circles). The dashed vertical lines mark the average lifetime values of 2.9 ps and 3.7 ps for **AuS-C12-TPD** and **AuS-C3-TPD**, respectively. The average TA signal lifetime τ_{av} is defined here as the time after which the normalized signal intensity drops to the value $\Delta OD(\tau_{av}) = e^{-1}$.

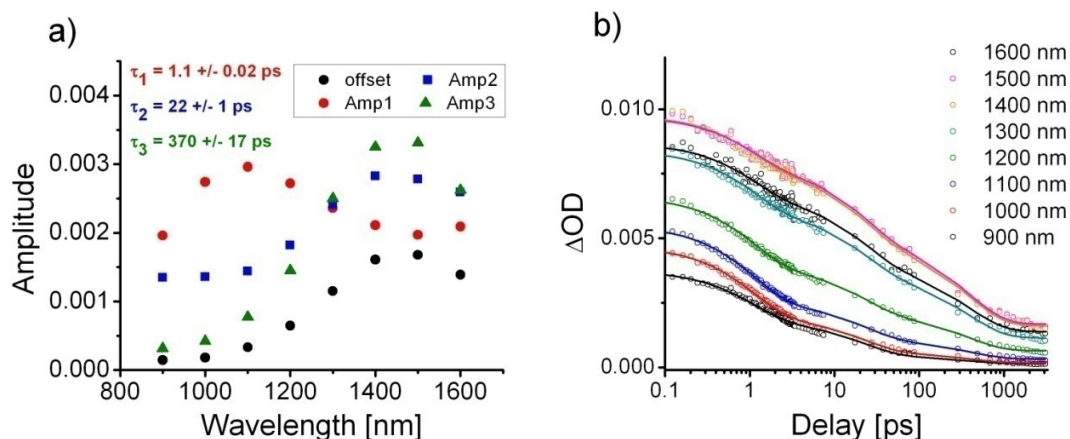


Fig. S14 a) Lifetimes and spectral distribution of preexponential amplitudes obtained by fitting the data acquired for a **C12-TPD** neat film with a sum of three exponential functions; b) kinetic traces (circles) and the corresponding curves from fitting the data (solid lines) with a sum of three exponential functions for the same sample as in a).

References

1. R. D. Hreha, Y.-D. Zhang, B. Domercq, N. Larribeau, J. N. Haddock, B. Kippelen and S. R. Marder, *Synthesis*, 2002, 1201-1212.
2. N. G. Andersen, S. P. Maddaford and B. A. Keay, *J. Org. Chem.*, 1996, **61**, 9556-9559.
3. R. A. Lampert, L. A. Chewter, D. Phillips, D. V. O'Connor, A. J. Roberts and S. R. Meech, *Anal. Chem.*, 1983, **55**, 68-73.
4. D. V. O'Connor and D. Phillips, *Time-correlated Single Photon Counting*, Academic Press Inc., London, 1984.
5. S. L. Logunov, T. S. Ahmadi, M. A. El-Sayed, J. T. Khoury and R. L. Whetten, *J. Phys. Chem. B*, 1997, **101**, 3713-3719.
6. S. Link and M. A. El-Sayed, *Annu. Rev. Phys. Chem.*, 2003, **54**, 331-366.
7. G. A. Rance, D. H. Marsh and A. N. Khlobystov, *Chem. Phys. Lett.*, 2008, **460**, 230-236.